

Variability, cycles, and trends of mean air temperature north of Colombia

Andrea Patricia MANRIQUE-CANTILLO^{1*} Enrique de Jesús MORALES-ACUÑA²
and Jean Rogelio LINERO-CUETO³

¹ Grupo de Investigación Suelo, Ambiente y Sociedad, Universidad del Magdalena, Carrera 32 No. 22-08, Santa Marta DTCH, Colombia.

² Departamento de Medio Ambiente, Centro Interdisciplinario para el Desarrollo Integral Regional, Instituto Politécnico Nacional, Unidad Sinaloa, Blvd. Juan de Dios Bátiz Paredes 250, Colonia San Joachín, 81101 Guasave, Sinaloa, México.

³ Facultad de Ingeniería, Universidad del Magdalena, Carrera 32 No. 22-08, Santa Marta DTCH, Colombia.

*Corresponding author; email: andreamanriquepc@unimagdalena.edu.co

Received: February 22, 2023; Accepted: September 15, 2023

RESUMEN

La variabilidad climática es de interés global debido a sus efectos socioeconómicos y ambientales sobre la población mundial. En Colombia, los cambios de temperatura afectan la seguridad alimentaria, especialmente para la población más vulnerable de la región Caribe. Analizamos la temperatura mensual del aire en la región nororiental colombiana (departamentos de Cesar, La Guajira y Magdalena). Se reconstruyeron series temporales con datos faltantes utilizando análisis de componentes principales no lineales. Posteriormente se evaluaron la variabilidad temporal, las asociaciones con eventos de variabilidad climática y las tendencias temporales. Los análisis de periodicidad indican el predominio de la variabilidad anual, aunque las asociaciones estadísticamente significativas con períodos de 3 a 7 años muestran la influencia de los eventos de El Niño-Oscilación del Sur (ENSO, por su sigla en inglés). El coeficiente de correlación de Spearman con $N = 360$ y una significancia de 95% muestra una mejor asociación con el Índice Multivariado de ENSO ($r_{sp\text{ medio}} = 0.38$) y el Índice de la Oscilación del Sur ($r_{sp\text{ medio}} = -0.32$). El análisis multianual mensual muestra tendencias positivas, con valores máximos entre marzo ($1.04^{\circ}\text{C mes}^{-1}$) y junio ($1.07^{\circ}\text{C mes}^{-1}$) en el valle del departamento de Cesar, y un mínimo en marzo, en el extremo norte de La Guajira ($0.2^{\circ}\text{C mes}^{-1}$).

ABSTRACT

Climate variability is of global interest due to its socioeconomic and environmental effects on the world's population. In Colombia, temperature changes affect food security, especially for the most vulnerable people in the Caribbean region. We analyzed monthly air temperature in northeastern Colombia (Cesar, La Guajira, and Magdalena departments). We reconstructed time series with missing data using nonlinear principal component analysis. Subsequently, temporal variability, associations with events of climatic variability, and temporal trends were evaluated. Periodicity analyses indicate the dominance of annual variability, although statistically significant associations with periods between 3 and 7 years show the influence of El Niño-Southern Oscillation (ENSO) events. The Spearman correlation coefficient with $N = 360$ and 95% significance shows a better association with the Multivariate ENSO Index ($r_{sp\text{ mean}} = 0.38$) and the Southern Oscillation Index ($r_{sp\text{ mean}} = -0.32$). The multi-year monthly analysis shows positive trends, with maximum values between March ($1.04^{\circ}\text{C month}^{-1}$), and June ($1.07^{\circ}\text{C month}^{-1}$) in the valley of the Cesar department, and a minimum in March, at the northernmost La Guajira ($0.2^{\circ}\text{C month}^{-1}$).

Keywords: air temperature, climate variability, Mann-Kendall test, trends, Colombian Caribbean region.1.

1. Introduction

Climate change and climate variability represent a risk for agriculture, food security, and the Colombian economy and society (Hodson et al., 2017). Evidence of climate change in Colombia has been described in several studies such as Pabón-Caicedo (2003), Vuille et al. (2003), Ochoa and Poveda (2008), Cantor-Gómez (2011), Carmona and Poveda (2014), and Hurtado-Montoya and Mesa-Sánchez (2015). Ramírez-Villegas et al. (2012) warn that by 2050 climate change will affect about 3.5 million people in Colombia, affecting 14% of the gross domestic product (GDP), corresponding to agriculture, employment, agro-industries, supply chains, and food and nutrition security. It is a priority to understand annual and interannual climate variability and its correlation with weather events in order to mitigate their negative impacts on national agricultural production (Barrios-Pérez et al., 2021).

Climate behavior based on meteorological variables such as precipitation and air temperature has been previously studied (Pabón-Caicedo et al., 2001). Studies in Colombia show that interannual variability of temperature responds to factors such as El Niño-Southern Oscillation (ENSO) (Poveda, 2004). Puertas-Orozco and Carvajal-Escobar (2008) evidence the correlation between air temperature and precipitation during ENSO events, with precipitation decreasing as air temperature increases, and also show that temperature varies with the physiography of the country.

In this sense, temperature correlates with NIÑO 3.4 and NIÑO 4 during December-January-February, and these correlations improve when considering the interannual variability (Puertas-Orozco and Carvajal-Escobar, 2008). León (2000) shows positive trends in maximum recorded temperatures, decreasing trends in mean temperature, and evidence of spectral frequencies with ENSO events, but this study used just one meteorological station in the northern Colombian region.

Mean annual temperatures in the Colombian Caribbean region range between 28 and 30 °C, except in the Sierra Nevada de Santa Marta (SNSM). The annual temperature cycle allows us to identify three seasons: (1) the warm season, with maximum temperatures from February to April, (2) the transition season, from June to August, and (3) the cold season,

with the lowest temperatures from September to November (Pabón-Caicedo et al., 2001).

Considering the evidence of climate change in Colombia, its impacts on agriculture, the economy, the health sector, food security, and the fact that studies carried out in northern Colombia used few stations to describe the spatial and temporal patterns of air temperature, it is necessary to evaluate the variability, cycles, and trends of mean air temperature in this region. Therefore, using historical temperature series from 24 meteorological stations distributed in three departments located in northern Colombia, this study seeks to contribute to the understanding of air temperature variability patterns in the Colombian Caribbean, the periods of oscillation of this variable, its relationship with climate variability indices, and temporal trends for a period of 30 consecutive years until 2020.

2. Study area

The Colombian Caribbean is divided into eight regions or departments (Meisel-Roca and Pérez-Valbuena, 2006). Seven of them are located in the continental Caribbean plain ending in the SNSM, which descends in the Guajira peninsula (Rangel-Buitrago and Anfuso-Melfi, 2013). The SNSM joins three departments in the northeastern Colombian Caribbean: Magdalena, Cesar, and La Guajira (between 8-11° N and 72-74° W) (Fig. 1), giving it distinctive features of relief and climate compared to the rest of the region (Meisel-Roca and Pérez-Valbuena, 2006). According to the Caldas-Lang classification of IDEAM (2015), the northern Colombian Caribbean is characterized by a dry climate in the low and flat parts. In mountainous areas, the climate varies from warm and humid to temperate and cold (IDEAM, 2011). In La Guajira, the northernmost part of South America, the climate is arid (IDEAM, 2011; Vanegas-Chamorro et al., 2015).

In the Department of Magdalena, the northeastern trade winds interact with the SNSM, creating a valley-mountain circulation that causes temperatures to drop in December, January, and February. In March, the heat is accentuated and humidity increases. In La Guajira maximum temperatures exceed 34 °C in June and August (Martín-Garzón, 2021). In the department of Cesar the average annual temperature

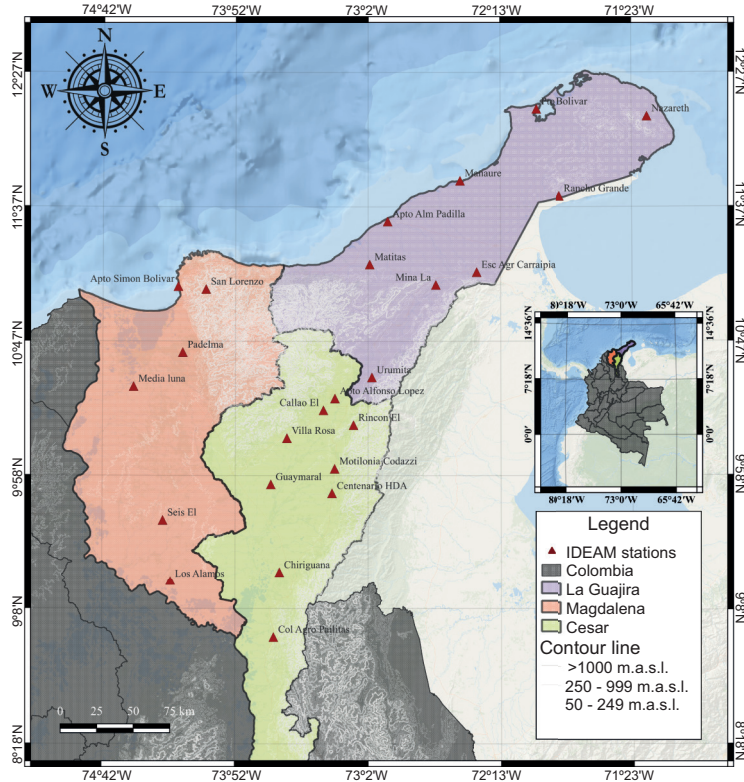


Fig. 1. Study area. Departments of La Guajira (purple), Cesar (yellow), and Magdalena (orange), and meteorological stations (red triangles). The description of the stations can be found in Table I.

exceeds 28 °C. Towards the foothills of the SNSM and the Serranía del Perijá (SP), the temperature has a relationship with altitude, which characterizes the Colombian mountains (IDEAM, 2015). The rainfall regime in Magdalena and Cesar is bimodal, with the first rainy season from April to May and the second one, more intense, from September to November. In La Guajira the rainfall is scarce and unevenly distributed, oscillating around 300 mm yr⁻¹ (IDEAM, 2015).

3. Methods

Monthly mean air temperature data (°C) from 24 meteorological stations (Fig. 1) were provided by the Instituto de Hidrología, Meteorología y Estudios Ambientales (IDEAM), available on the website <http://dhime.ideam.gov.co/atencionciudadano/>. Table I describes in detail the characteristics of the stations used.

A quality control was carried out to verify the reliability of the datasets, considering the number of missing data in each of the time series and their temporal length. Time series with three or more months missing were excluded. As a result, 24 were available for the departments of Magdalena, Cesar, and La Guajira. Nonlinear principal component analysis (NLPCA) was used to complete the missing data in each time series, parametrized with a circular inverse model. The network is trained in 1500 iterations (Scholz et al., 2005).

A circular unit at the component layer is introduced to the NLPCA, which describes a potential circular data structure by means of closed curve, to obtain circular components. The auto-associative neural network contains a circular unit pair (p , q) in the component layer, and the output values z_p and z_q (Eq. [1]) are constrained to lie on a unit circle represented by a single angular variable θ (Scholz, 2007).

Table I. Main characteristics of the selected IDEAM meteorological stations (name, selected abbreviation, time length, category, latitude, longitude, and altitude).

Regions	Code	Station	Abbreviation	Time length	Category	Latitude (°)	Longitude (°)	Altitude (masl)
Cesar	28035030	Apto. Alfonso López	ALFONS	1991 - 2020	SP	10.44	-73.25	138
	28035020	El Callao	CALLAO	1987 - 2020	CO	10.36	-73.32	110
	28025090	Centenario HDA	CENTEN	1979 - 2020	CO	9.85	-73.27	100
	25025250	Chiriguana	CHIRIG	1985 - 2020	CO	9.36	-73.59	40
	25025330	Col. Agro Pailitas	COLAGR	1987 - 2020	CP	8.95	-73.63	50
	28035040	Guaymaral	GUAYMA	1987 - 2020	CO	9.9	-73.65	50
	28025070	Motilonia Codazzi	MOTILO	1973 - 2020	AG	10	-73.25	180
	28025020	El Rincón	RINCON	1964 - 2020	CO	10.27	-73.13	350
	28035010	Villa Rosa	VILARO	1985 - 2020	CO	10.19	-73.55	70
	15065010	Apto. Alm. Padilla	ALMIRA	1991 - 2020	SP	11.53	-72.92	4
La Guajira	15085030	Esc. Ag.r Carraipia	ESCAGR	1968 - 2020	CO	11.22	-72.36	118
	15075030	Manaure	MANAUR	1991 - 2020	CP	11.78	-72.46	1
	15045010	Matitas	MATITA	1964 - 2020	CO	11.26	-73.03	20
	15065130	La Mina	MINALA	1990 - 2020	CP	11.14	-72.62	80
	15085020	Nazareth	NAZARE	1972 - 2020	CP	12.18	-71.28	85
	15075060	Pto. Bolívar	PBOLIV	1986 - 2020	CP	12.22	-71.98	10
	15085040	Rancho Grande	RANCHO	1971 - 2020	CO	11.69	-71.83	50
	28015070	Urumita	URUMIT	1978 - 2020	CO	10.57	-73.02	255
	15015050	Apto. Simón Bolívar	ASIMBO	1952 - 2020	SP	11.13	-74.23	4
	25025320	Los Álamos	LALAMO	1987 - 2020	CP	9.3	-74.27	25
Magdalena	29065080	Media Luna	MELUNA	1985 - 2020	CP	10.51	-74.51	20
	29065020	Padelma	PADELM	1967 - 2020	CO	10.72	-74.2	20
	25025300	El Seis	SEISEL	1987 - 2020	CO	9.68	-74.32	50
	15015060	San Lorenzo	SLOREN	1969 - 2020	CP	11.11	-74.05	2200

CO: ordinary climatological; SP: main synoptic; CP: main climatological; AG: agrometeorology.

$$z_p = \cos(\theta) \text{ and } z_q = \sin(\theta) \quad (1)$$

$$\frac{\partial E}{\partial \omega_{pm}} = \sum_n \sigma_p^n z_m^n \quad \text{and} \quad \frac{\partial E}{\partial \omega_{qm}} = \sum_n \sigma_q^n z_m^n \quad (3)$$

The forward propagation is represented by:

$$a_p = \sum_m \omega_{pm} z_m \quad \text{and} \quad a_q = \sum_m \omega_{qm} z_m \quad (2)$$

where z_m are sums of their inputs given weights (ω_{pm} and ω_{qm}) for the matrix. For backward propagation, we need the derivatives of the error function remaining for all n samples to be:

With the reconstructed series, the annual and semi-annual variability was analyzed using monthly climatology and boxplot diagrams.

To evaluate the performance of the missing data reconstruction method (NLPCA), we used the Spearman correlation coefficient (r_{sp}) (Eq. [4]) (Spearman, 1904; Zar, 1972) with a 95% significance. Mean

absolute error (MAE) (Eq. [5]), and bias (Eq. [6]) are employed in the paired comparisons between the reconstructed and original time series.

$$r_{sp} = 1 - \frac{6 \sum_{i=1}^n D^2}{N(N^2 - 1)} \quad (4)$$

$$MAE = \frac{\sum_{i=1}^n |ts_r - ts_o|}{n} \quad (5)$$

$$bias = \frac{\sum_{i=1}^n (ts_r - ts_o)}{\sum_{i=1}^n ts_o} \quad (6)$$

In these equations, D is the difference between the ranks of two samples, N the number of ranks, ts_r is the reconstructed time series, ts_o represents the original time series, and n is the total number of data.

The critical value (r_c) for the Spearman correlation (Eq. [7]) is calculated from the following expression:

$$r_c = r_{sp} \sqrt{N - 1} \quad (7)$$

where the hypothesis test is given by:

$$\begin{cases} H_0: \text{No correlation exists if } r_c > r_{sp} \\ H_1: \text{Correlation exists if } r_c < r_{sp} \end{cases} \quad (8)$$

The WMO recommends using the most recent 30-year period ending in a year ending in 0 for the calculation of the climate normal for the current period from 01/01/1991 to 31/12/2020 (WMO, 2017). Therefore, the time series are cut for this period. The time series periodicities were evaluated using the cyclic descent technique (Bloomfield, 1996), and implemented with the tool developed by González-Rodríguez et al. (2015). This technique consists of decomposing the time series to detect the most important frequency, phase, and amplitude, as well as statistically significant harmonics.

$$X_e = \alpha + \beta t + \sum_{i=1}^m \left(a_i \cdot \cos(2\pi p_i^{-1}) + b_i \cdot \sin(2\pi p_i^{-1}) \right) \quad (9)$$

where α and β are the linear regression coefficients when a linear trend is assumed (otherwise both parameters equal zero), and a_i , b_i and p_i are the

corresponding parameters of the i th harmonic. Thus, a_i and b_i are used to calculate the amplitudes and phase angles.

If a linear trend exists in the time series, its magnitude can be quantified using Sen's (1968) non-parametric slope estimator:

$$\beta = mediana \left(\frac{x_j - x_i}{j - i} \right) \quad (10)$$

where β represents the slope mean values between data measurements x_j and x_i at time steps j and i , respectively, with $j > i$. The positive value of β indicates an increasing trend while its negative value indicates a decreasing trend. The direction of the data trend is indicated by the sign of β , while its slope is determined by its value. By comparison to linear regression, this technique offers the benefit of constraining the impact of missing data or outliers on the slope.

To establish a relationship between the mean temperature at the 24 selected stations and some climate variability indices, non-parametric correlations were performed using Spearman's coefficient (r_{sp}) (Eq. 4) and the hypothesis test given in Eq. (8). The variability indices used are the Southern Oscillation Index (SOI), which is a standardized index based on the observed sea level pressure (SLP) differences between Tahiti and Darwin, Australia (NOAA, 2005a); the Multivariate ENSO Index (MEI v2), which is a bi-monthly time series that represents the combined empirical orthogonal function (EOF) of five variables: SLP, sea surface temperature (SST), zonal and meridional components of surface wind, and outgoing longwave radiation (OLR) over the tropical Pacific basin (30° S- 30° N, 100° E- 70° W) (Wolter and Timlin, 2011; NOAA, 2018). The North Atlantic Oscillation (NAO) index relies on the surface SLP difference between the Subpolar Low and the Subtropical (Azores) High. A positive NAO phase signifies pressure and height anomalies that are below average across the North Atlantic high latitudes and above average across the central North Atlantic, western Europe, and the eastern United States (NOAA, 2005b). The sunspot number is an index of the activity of the entire visible disk of the sun. It is determined each day without reference to preceding days and determined by the sunspot group, and it may consist of one or a large number of distinct spots of different sizes (Künzel, 1962; SILSO, 2015).

Two non-parametric techniques, the modified Mann-Kendall test (Hamed and Rao, 1998) and the Theil-Sen estimator (Theil, 1950; Sen, 1968), also used in works such as Dahmen and Hall (1990) and Morales-Acuña et al. (2019), were used to calculate the monthly mean temperature trend and multi-year monthly averages.

The modified Mann-Kendall test offers an alternative for detecting trends in time series that have autocorrelation with the difference in the formula to calculate variance (Morales-Acuña et al., 2021):

$$Var(S)^* =$$

$$\left(\frac{n(n-1)(2n+5) - \sum_{i=1}^m t_i(t_i-1)(2t_i+5)}{18} \right) \frac{n}{n^*} \quad (11)$$

where $Var(S)^*$ is the modified variance, n the number of observations, m the number of data pairs in the series, and t_i the number of ties at the timestep i . Thus n/n^* (Eq. 12) is the correction factor given by r_k^R , corresponding to the lag-k autocorrelation coefficient of the ranks of the data:

$$n/n^* = 1 + \frac{2}{n(n-1)(n-2)} \sum_{j=1}^{n-1} (n-k)(n-k-1)(n-k-2)r_k^R \quad (12)$$

The significance of the trend is determined with Eq. (13):

$$\begin{cases} Z = \frac{S-1}{\sqrt{Var(S)^*}} & \text{if } S > 0 \\ Z = 0 & \text{if } S = 0 \\ Z = \frac{S+1}{\sqrt{Var(S)^*}} & \text{if } S < 0 \end{cases} \quad (13)$$

4. Results

The mean air temperature time series were reconstructed with 95% reliability to complete the missing data, with a mean correlation coefficient of 0.99 and a mean absolute error of 1.8×10^{-4} °C. The performance of this technique is shown in Figure 2.

The analysis of the annual cycle (Fig. 3) allowed us to identify that the stations located in the department of Cesar (Fig. 3a-i) are characterized by a bimodal behavior, in which the stations have their highest maximum temperature in March and the second maximum temperature occurs in July. Temperature ranges from 27 to 31 °C. Likewise, the minimum of maximum temperatures is found at the RINCON station (350 masl) (Fig. 3h) located at the foothills of the SP.

The behavior in La Guajira is mostly unimodal (Fig. 3j-r). The highest temperatures occur mostly in

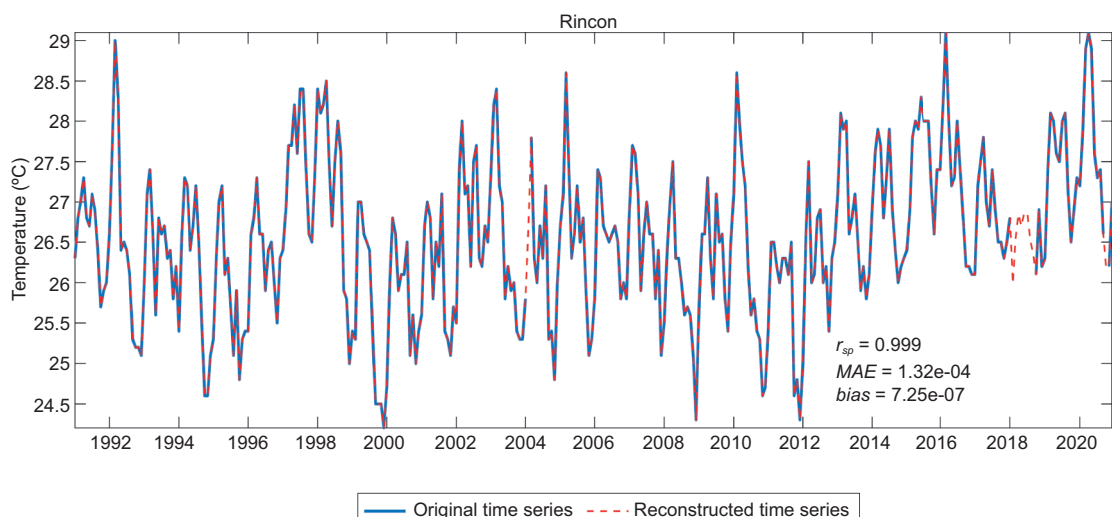


Fig. 2. Reconstruction of time series by the NLPICA method and statistical metrics between the original and the reconstructed time series of RINCON station (department of Cesar). The results of the time series reconstruction are shown in full in the supplementary material (Figs. S1-S3).

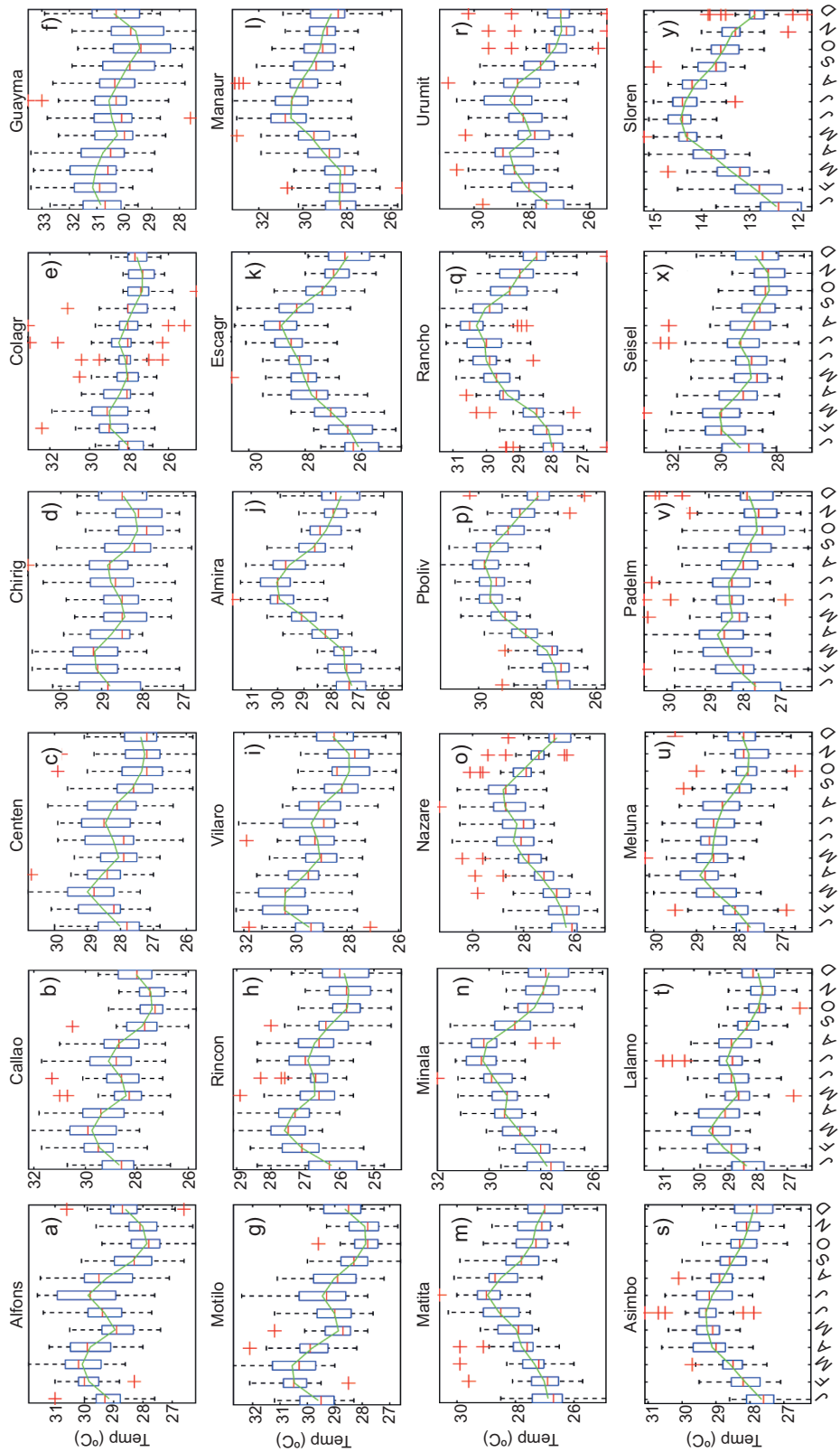


Fig. 3. Monthly climatology of air temperature in the departments of (a-i) Cesar, (j-r) La Guajira, and (s-y) Magdalena for the period 1991-2020. The green line is the monthly mean. Red crosses are outliers.

June-July-August; however, the department can be divided into two zones: north and center-south. In the first one, all stations obey this behavior except NAZARE (Fig. 3o), which has a minor first high temperature in June. Also, URUMIT (Fig. 3r) in the south of the department has a similar behavior to stations in the Cesar department, since it has two maximum temperatures in April and July (approximately 29 °C).

The department of Magdalena (Fig. 3s-y) is divided into north, center-south, and mountain zones (Fig. 3y). The north-center fraction is formed by a station in the coastline (ASIMBO, Fig. 3s), which is unimodal with a maximum temperature of ~ 29 °C in May. The station with highest altitude and lowest maximum temperature is SLOREN (2200 masl) (Fig. 3y), located in the foothills of the SNSM; it has a unimodal behavior with maximum temperature in July and minimum high temperature. In this station, the super humid cold weather predominates, and temperatures fluctuate between 12.5 and 14.5 °C. The center-south fraction has a bimodal behavior, within which the stations located at the center (PADELM, Fig. 3v, and MELUNA, Fig. 3u) have their first highest maximum in April and the second in July. The stations further south in the department (SEISEL, Fig. 3x, and LALAMO, Fig. 3t) have a highest maximum temperature in March of ~ 29 °C, and a second maximum temperature in July with an average of 27.4 °C.

The periodicity analysis (Table II) allowed us to identify from the five significant harmonics that air temperature variability responds mainly to the annual cycle, except for CHIRIG, located in the valley of Cesar, where the highest significance corresponds to a ~ 6-years cycle and the annual cycle in the fifth harmonic. For the second harmonic, the stations are influenced by semi-annual periods (22%), and periods of 3-7 years (16%) and more than 12 years (28%). In the third, fourth, and fifth harmonics, 3-7 years periodicities predominate with 38%, 56%, and 34% of occurrence, respectively.

For all stations, the Spearman correlation mean coefficient with 95% of significance and $N = 360$ is greater than the critical value ($r_c = 0.103$) rejecting the null hypothesis. In this respect, it is shown that there is a better association with the MEI (83%), SOI (75%), and sunspot (25%).

The correlation with the MEI (Fig. 4b) is mostly significantly moderate in Cesar (13%) and La Guajira (13%), with a correlation coefficient of $r_{sp} = 0.66$. The northern region of Cesar and central Magdalena have a high positive correlation (4%) and a moderate positive correlation (17%). The correlation with the SOI (Fig. 4a) is inverse, mostly with low correlation in Cesar (17%) and La Guajira (17%) with $r_{sp} = -0.28$ and moderate correlation in Cesar (13%) and La Guajira (13%), with $r_{sp} = -0.39$. The strongest signals of correlation with SOI are in the coast of Magdalena, SNSM, and the north part of Cesar.

It can be said that with 95% confidence there is no relationship with the NAO (Fig. 4c). The negative correlation that exists is very low, localized in the coast of Magdalena, in the northern part of La Guajira, and near Urumita. A similar situation occurs with sunspots (Fig. 4d) and mean air temperature, since there is no relationship. The signal is negative very low and occurs in the foothills of the SNSM towards La Guajira.

The trend in all stations is positive, indicating an increase in temperature. The maximum trend in full series (Fig. 5) is recorded in the department of Cesar at the GUAYMA station, with $0.07 \text{ }^{\circ}\text{C yr}^{-1}$. This is followed by the maximum in the department of Magdalena at the PADELM station, with $0.05 \text{ }^{\circ}\text{C yr}^{-1}$, both between 20-50 masl. Lesser positive trends ($0.02 \text{ }^{\circ}\text{C yr}^{-1}$) in ASIMBO and LALAMO (Magdalena), and $0.01 \text{ }^{\circ}\text{C yr}^{-1}$ in RANCHO (La Guajira) are found.

Similarly, the monthly multiannual trend analysis (Fig. 6) shows positive values in all months, ranging between 0.2 and $1.07 \text{ }^{\circ}\text{C yr}^{-1}$. The maximum positive trends occur most of the year in the center of Cesar (GUAYMA reaching $1.07 \text{ }^{\circ}\text{C yr}^{-1}$ in June); however, January ($0.72 \text{ }^{\circ}\text{C yr}^{-1}$) and August ($0.68 \text{ }^{\circ}\text{C yr}^{-1}$) the maximum positive trends occur in PADELM (northeast of Magdalena). The minimum trends occur in March in RANCHO ($0.2 \text{ }^{\circ}\text{C yr}^{-1}$). Minimum trends occur in January near the coast of Magdalena (ASIMBO, $0.32 \text{ }^{\circ}\text{C yr}^{-1}$), and between February and May, July-August and October-November in mountain foothills. In the north coast of La Guajira, the minimum trends occur in the PBOLIV station (June and September, with 0.28 and $0.38 \text{ }^{\circ}\text{C yr}^{-1}$, respectively) and NAZARE (December, with $0.27 \text{ }^{\circ}\text{C yr}^{-1}$).

Table II. Periodic regression analysis of the time series of each station using the cyclic descent technique (Bloomfield, 1996), and implemented with the tool developed by González-Rodríguez et al. (2015)*.

Regions	Station	Abbreviation	Amplitudes					Periods				
			1	2	3	4	5	1	2	3	4	5
Apto. Alfonso												
Cesar	López	ALFONS	0.82	0.52	0.39	0.37	0.36	1.0	0.5	13.1	3.0	5.6
	El Callao	CALLAO	0.84	0.54	0.53	0.49	0.31	1.0	0.5	14.7	5.9	4.3
	Centenario											
	HDA	CENTEN	0.61	0.45	0.41	0.37	0.35	1.0	13.4	5.8	0.5	3.0
	Chiriguana	CHIRIG	0.35	0.34	0.33	0.32	0.30	5.7	4.0	0.5	15.5	1.0
	Col. Agro											
	Pailitas	COLAGR	0.59	0.55	0.42	0.32	0.30	1.0	5.7	0.5	3.1	4.0
	Guaymaral	GUAYMA	0.61	0.45	0.39	0.33	0.29	1.0	13.4	0.5	7.6	5.7
	Motilonia											
	Codazzi	MOTILO	0.99	0.66	0.48	0.32	0.25	1.0	0.5	5.8	3.0	12.8
La Guajira	El Rincón	RINCON	0.71	0.38	0.38	0.30	0.28	1.0	0.5	5.8	4.5	15.5
	Villa Rosa	VILARO	0.95	0.59	0.43	0.36	0.31	1.0	0.5	15.5	5.8	3.1
Apto. Alm.												
Padilla	ALMIRA	1.30	0.45	0.31	0.26	0.24	1.0	14.3	0.5	3.0	4.3	
Esc. Ag.r												
Carraipia	ESCAGR	1.20	0.39	0.36	0.18	0.18	1.0	15.5	6.6	3.8	0.5	
Manaure	MANAUR	1.06	0.46	0.37	0.33	0.31	1.0	12.9	5.6	7.2	2.9	
Matitas	MATITA	0.89	0.37	0.24	0.23	0.23	1.0	12.3	4.3	3.5	2.9	
La Mina	MINALA	1.18	0.53	0.35	0.33	0.31	1.0	14.5	5.7	2.9	1.5	
Nazareth	NAZARE	1.16	0.35	0.32	0.31	0.24	1.0	4.3	10.0	3.5	2.9	
Pto. Bolívar	PBOLIV	1.22	0.43	0.29	0.21	0.20	1.0	15.5	11.6	2.8	3.6	
Rancho												
Magdalena	Grande	RANCHO	1.06	0.32	0.23	0.22	0.22	1.0	2.8	1.5	7.3	3.5
	Urumita	URUMIT	0.78	0.49	0.40	0.37	0.31	1.0	5.5	0.5	3.0	10.5
Apto. Simón												
Bolívar	ASIMBO	0.75	0.32	0.25	0.21	0.19	1.0	13.7	4.3	3.0	10.5	
Los Álamos	LALAMO	0.61	0.36	0.26	0.26	0.22	1.0	0.5	3.0	14.6	2.5	
Media Luna	MELUNA	0.51	0.36	0.26	0.25	0.21	1.0	11.7	5.6	15.5	3.0	
Padelma	PADELM	0.43	0.40	0.36	0.31	0.27	1.0	7.7	4.6	5.5	10.5	
El Seis	SEISEL	0.61	0.48	0.45	0.35	0.35	1.0	11.5	0.5	6.3	15.5	
San Lorenzo	SLOREN	0.85	0.18	0.18	0.13	0.12	1.0	0.5	3.7	6.1	3.0	

*Amplitude and periods of the first five with statistical significance of 95% with $0.31 < R^2 \leq 0.73$.

5. Discussion

The reconstruction of mean air temperature time series from the inverse NLPCA approach (Fig. 2) allowed us to identify that the extraction of the nonlinear components from the incomplete time series and its subsequent nonlinear mapping achieved an adequate reconstruction of the analyzed time series. Although the reconstructed series slightly overestimate the mean values, the variability of the original series is preserved, as reported by other authors

when reconstructing time series of different variables (Ruessink et al., 2004; Barakzehi et al., 2013; Canchala et al., 2020; Morales-Acuña et al., 2021).

The analysis of monthly air temperature climatologies in the Colombian Caribbean (Fig. 2) identified a heterogeneous distribution in terms of mean air temperature values, such that a warm season with maximum temperatures in July was identified in the department of La Guajira, while two warm seasons with maximum temperatures in April and July were

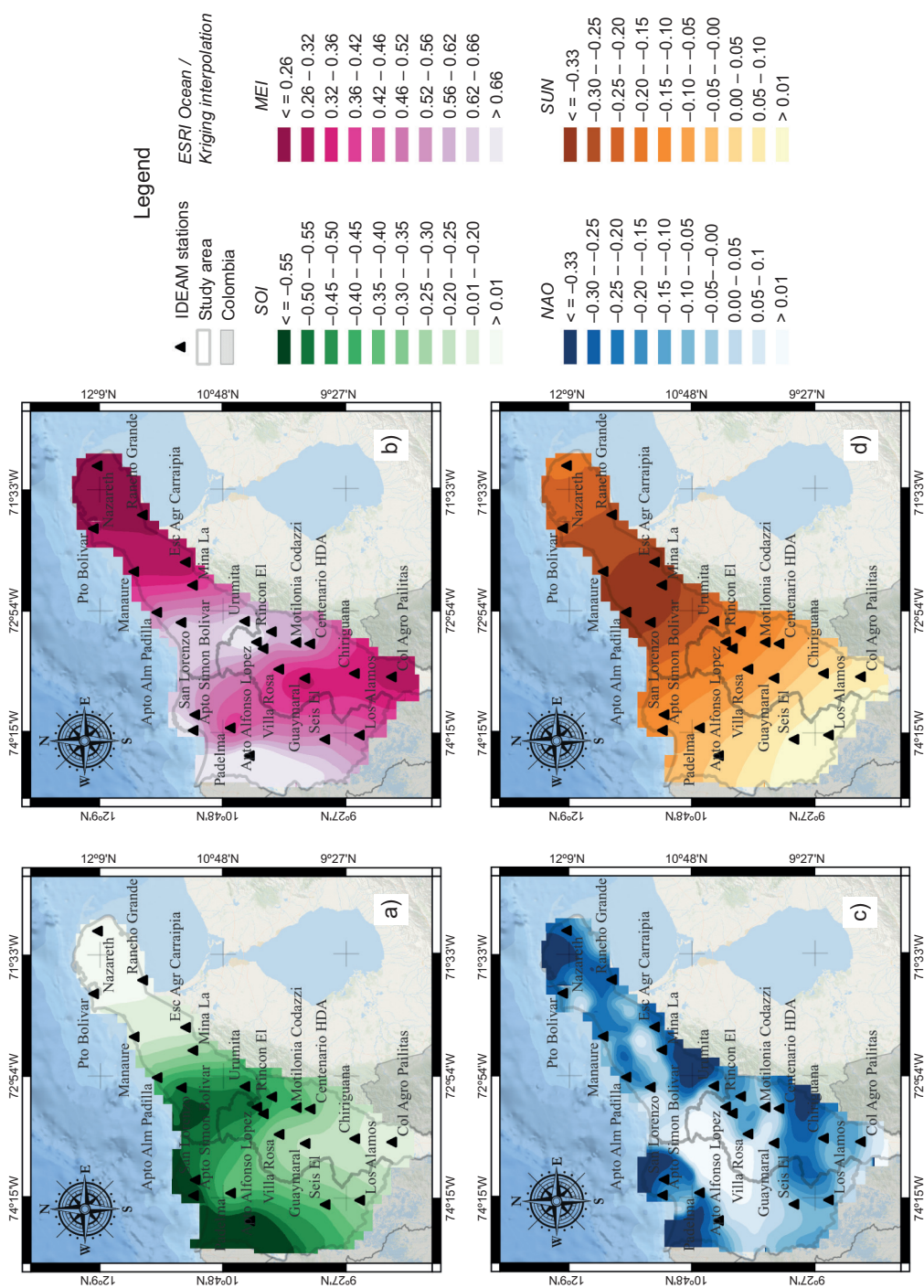


Fig. 4. Spearman's correlation coefficient (95% significance, and critical value of ± 0.103) between air temperature and (a) SOI, (b) MEI, (c) NAO, and (d) Sunspot index.

found in the department of Cesar. In Magdalena, due to the presence of the SNSM, the proximity to the Caribbean Sea, the extensive plains located in the center of the department, and its interaction to the south with the La Mojana region, a warm season

with maximum in May and July was characterized for the coastal region and the SNSM, while in the plains of the central region two warm seasons with maximum in April and July were observed and in the southern region two warm seasons with maximum in

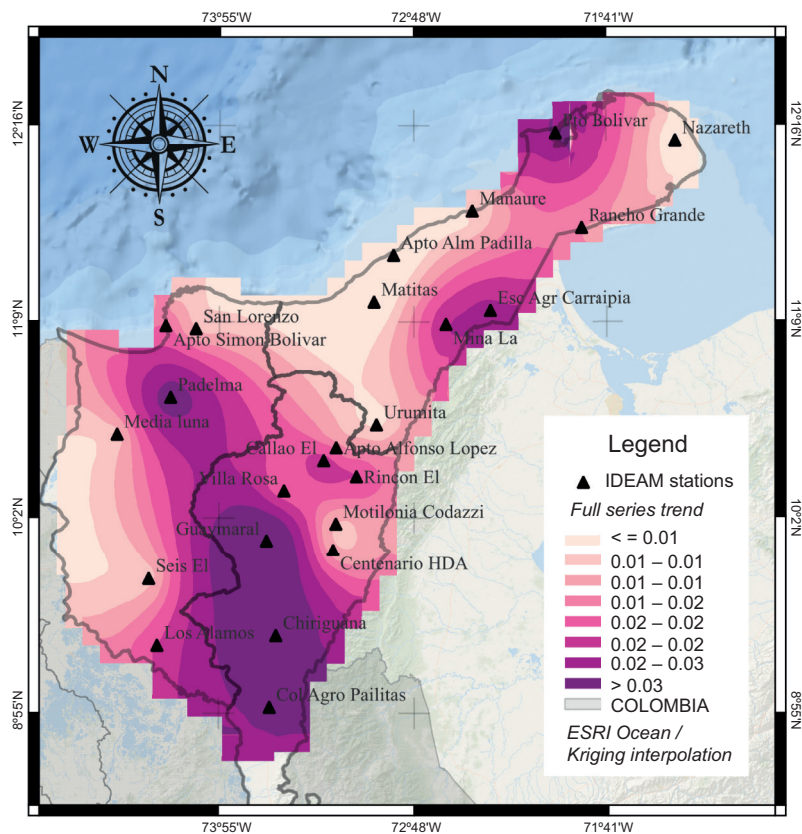


Fig. 5. Trend analysis ($^{\circ}\text{C yr}^{-1}$) of average temperature of the full series.

March and July were identified. This heterogeneous distribution of air temperature responds to regional differences due to latitude, topography, mountain range orientation, and the average vertical temperature gradient ($5.53\text{ }^{\circ}\text{C km}^{-1}$) reported by Eslava (1992) for all of Colombia. In addition, the seasons and heterogeneity found in the present study coincide with those reported by Pabón-Caicedo et al. (2001), who established a heterogeneous distribution in the mean values of air temperature for three stations evaluated in the Colombian Caribbean.

One of the relevant factors in the annual temperature cycle of the Colombian Caribbean is the Caribbean Low-Level Jet (CBNC) (Amador-Astúa, 1998), which has been related to trade wind fluctuations, increased hurricane activity, and increased temperature in northern South America (Yepes et al., 2019). This low-level jet in the Caribbean converges with the Northern Hemisphere summer (Amador-Astúa, 1998; Serna et al., 2018) and with the temperature maxima

reported in this study. In addition to this low-level jet, one of the main intra-annual modulators of climate in Colombia is the Intertropical Convergence Zone (ITCZ) (León et al., 2000), which has a presence in the Colombian Caribbean, specifically during July. These two intra-annual scale phenomena coincide with the periods of one year and ~ 6 months present in the first and second harmonics calculated in our study from the cyclic descent analysis (Table II). This same analysis allowed us to identify periods between 3 and 7 years that are in agreement with ENSO oscillation periods (Rasmusson et al., 1990), periods > 10 years that coincide with solar magnetic activity (Friis-Christensen and Lassen, 1991, 1994; Connolly et al., 2021; Velasco-Herrera et al., 2021). Both phenomena directly influence the climate on interannual scales, but there is evidence that during ENSO years, the CBNC and the ITCZ are affected (Builes-Jaramillo et al., 2023), which reflects on air temperature in the Colombian Caribbean.

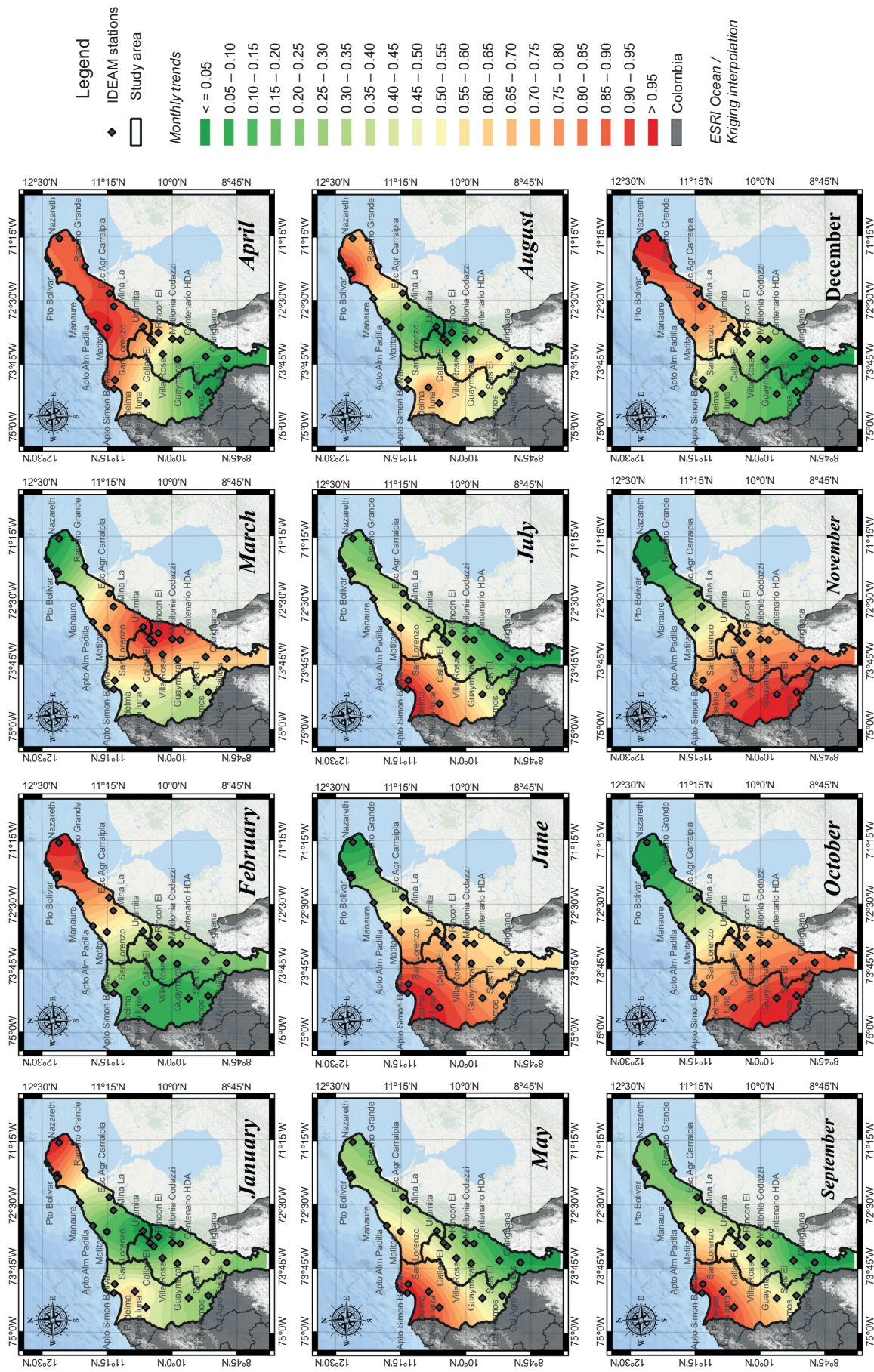


Fig. 6. Trend analysis ($^{\circ}\text{C yr}^{-1}$) of monthly average temperature.

The evaluation of the effects of climate variability events on air temperature in the Colombian Caribbean was approached in this work by means of associations between time series of air temperature and the SOI, MEI, NAO, and Sunspot climate indices (Fig 3). The MEI was considered the most influential factor in air temperature fluctuations, with a statistical significance of 95% and a Spearman's correlation coefficient average value of 0.37, followed by the SOI ($r_{sp} = -0.31$). The NAO did not present significant statistical associations, hence its effects are not considered relevant to air temperature fluctuations in the Colombian Caribbean. An entropy analysis between MEI and SOI performed by Ortiz-Tánchez et al. (2002) revealed different characteristics of both ENSO quantifiers, being the MEI index the one that shows quantitative evidence of mid-range correlations to the Southern Oscillation, since it presents a more constructive effect of its fluctuations in comparison with those of the SOI, which clearly established the onset of El Niño/La Niña and its effects beyond one month. In this sense, the MEI index behaves much better than the SOI in the description and predictability of ENSO, as we found in the study of its effects on air temperature in the Colombian Caribbean from the correlation coefficients and harmonics 3, 4 and 5. In addition to this, in the present study we were able to determine ENSO as the main influential factor in climate variability on an interannual scale, as has been reported in different regions of the world and some regions of Colombia (e.g., Pabón-Caicedo et al., 2001; Rodríguez-Rubio, 2013). Finally, although a significant influence of solar magnetic activity on climate variability has been reported (Buendía-Carrera et al., 2012), for the Colombian Caribbean we found a low correlation statistically significant at 95%, indicating that although the influence of this phenomenon is not relevant, it is of vital importance to consider it in studies of climate teleconnections.

The evaluation of climate goes hand in hand with its tendencies, for which in the present study we determined for the Colombian Caribbean, based on non-parametric statistical techniques, that in the department of Cesar the average air temperature is increasing $\sim 0.01^{\circ}\text{C yr}^{-1}$ more than in the departments of Magdalena and Guajira (Fig. 5). Carmona and Poveda (2014) reported overall increases in mean air temperature in the Colombian Caribbean

region after evaluating the trend of hydro-climatic variables throughout Colombia; they determined that 87% of the monthly minimum temperature series assessed presented increases between 0.01 and $0.08^{\circ}\text{C yr}^{-1}$. In this sense, according to the Third National Communication on Climate Change (TCNCC) of Colombia (IDEAM, 2017), based on IPCC reports, the average temperature may increase $\sim 1^{\circ}\text{C}$ by 2040 with respect to the reference period 1976-2005 in the northern region of the country. The increasing trends found in this study may be related to the migration of inhabitants from rural regions to cities due to forced displacement, changes in land use, and desertification processes to which the Colombian Caribbean is being subjected. Therefore, in this region in particular, the growing trend could be related to an urban heat island effect, as mentioned by Jones et al. (1990). In addition to overpopulation and changes in land use, increases in greenhouse gas emissions due to vehicle growth (Lamb et al., 2021) could be another factor causing atmospheric warming and the increases in air temperature reported in this study.

Analyses of global trends conducted by trimesters, decades, or seasons indicate positive temperature trends associated with higher temperatures and therefore major impacts on the agricultural sector, which is considered by some as evidence of climate change (Al-Buhairi, 2010; El-Geziry, 2022; Mateus and Potito, 2022; De et al., 2023). Finally, the presence of aerosols and particles of terrigenous origin from the Guajira deserts reported by Orozco-Rodríguez (2021) and from the Sahara Desert (Hernández, 2014; Poleo and Briceño, 2014), could be affecting the energy balance in such a way that the reduction of incoming solar radiation to the surface (Slingo et al., 2006) increases daily heating rates (Chen et al., 2017), warming of the middle troposphere, and cooling of the lower troposphere (Mohalfi et al., 1998), all of which could cause increases in air temperature in the Colombian Caribbean, as we report in the present study. Finally, the results obtained in this work on the spatial heterogeneity of mean air temperature values, the influence of the CBNC, the suitability of evaluating the effects of ENSO with the MEI index, and the positive trends, provide climate change scenarios that should be taken into account for the development of management plans aimed at thermal comfort, reduction of greenhouse gas emissions, and

land use, thus favoring the environmental conditions of the Colombian Caribbean, its inhabitants, and the different species that coexist in it.

6. Conclusion

The analysis of the variability, cycles, and trends of mean air temperature in the Colombian Caribbean, based on data from IDEAM meteorological stations, allowed establishing that the reconstruction of time series by the NLPCA method guarantees the variability and mean values of air temperature in this region, such that the comparison metrics present mean values of 0.99, 1.8×10^{-4} and $3.5 \times 10^{-7} ^\circ\text{C}$ for Spearman's correlation coefficient, mean absolute error, and bias. In addition, it was identified that the annual cycle of air temperature shows heterogeneity between the mean values and their spatial distribution, mainly due to the geographical position, orography, proximity to the sea, and humidity contributions of the continental environments belonging to this region.

The periodicity analysis established that the main modes of variability at the intra-annual scale are the CBNC and the ZCIT, while at a global scale ENSO predominated, which in turn showed better correlations than the other modes of climatic variability evaluated in order to identify the influence on air temperature fluctuations. This association analysis allowed us to characterize the MEI index as the most suitable for evaluating the effects of this mode of variability on air temperature.

Finally, the trends of the complete series oscillate between 0.01 and $0.07 ^\circ\text{C yr}^{-1}$, with a maximum in the department of Cesar. As for the monthly trends for the study period (1991-2020), it had a maximum between March and June in the department of Cesar ($1.07 ^\circ\text{C yr}^{-1}$) and a minimum in La Guajira ($0.2 ^\circ\text{C yr}^{-1}$) in March. These temperature increases are significant given the productive activities of crops and livestock in the region, which may be affected by them as well as by periods of drought and water resource availability. The results obtained in this study are very useful for decision-makers when considering the average air temperature variable, its variability, cycle, and trends, and therefore its effects on heat islands that currently exist in the population centers associated with the economic activities that

take place in the region, thus allowing them to establish management plans aimed at thermal comfort and climate change mitigation measures.

Acknowledgments

The authors thank the Instituto de Hidrología, Meteorología y Estudios Ambientales (IDEAM) for providing the necessary data to carry out this study. We also thank the research group Suelo, Ambiente y Sociedad of the Universidad del Magdalena for their support in the loan of computer equipment. Morales-Acuña (CVU No. 588798) thanks the scholarship program for a postdoctoral stay in Mexico 2022 in the modality by incidence.

References

- Al-Buhairi MH. 2010. Analysis of monthly, seasonal and annual air temperature variability and trends in Taiz City—Republic of Yemen. *Journal of Environmental Protection* 1: 401-409. <https://doi.org/10.4236/jep.2010.14046>
- Amador-Astúa, JA. 1998. A climate feature of the tropical Americas: The trade wind easterly jet. *Tópicos Meteorológicos y Oceanográficos* 5: 91-102. Available at: <https://hdl.handle.net/10669/76623> (accessed 2023 May 11).
- Barakzehi M, Amirshahi SH, Peyvandi S, Afjeh MG. 2013. Reconstruction of total radiance spectra of fluorescent samples by means of nonlinear principal component analysis. *Journal of the Optical Society of America A* 30: 1862-1870. <https://doi.org/10.1364/JOSAA.30.001862>
- Barrios-Pérez C, Okada K, Garcés-Varón G, Ramírez-Villegas J, Rebollo MC, Prager SD. 2021. How does El Niño Southern Oscillation affect rice-producing environments in central Colombia? *Agricultural and Forest Meteorology* 306: 108443. <https://doi.org/10.1016/j.agrformet.2021.108443>
- Bloomfield P. 1996. Fourier analysis of time series: An introduction. 2nd ed. John Wiley and Sons, New York.
- Buendía-Carrera EJ, Patiño R, Salas A. 2012. Secuencia de la circulación de las Ondas del Este y las lluvias del año 2010 en Colombia y Venezuela. *Ingeniería de Recursos Naturales y del Ambiente* 11: 107-116. Available at <https://www.redalyc.org/articulo.oa?id=231125817010> (accessed 2022 July 25).

- Builes-Jaramillo A, Valencia J, Salas HD. 2023. The influence of the El Niño-Southern Oscillation phase transitions over the northern South America hydroclimate. *Atmospheric Research* 290: 106786. <https://doi.org/10.1016/j.atmosres.2023.106786>
- Canchala T, Alfonso-Morales W, Carvajal-Escobar Y, Cerón WL, Caicedo-Bravo E. 2020. Monthly rainfall anomalies forecasting for southwestern Colombia using artificial neural networks approaches. *Water* 12: 2628. <https://doi.org/10.3390/w12092628>
- Cantor-Gómez D. 2011. Evaluación y análisis espaciotemporal de tendencias de largo plazo en la hidroclimatología colombiana. M.Sc. thesis. Universidad Nacional de Colombia.
- Carmona AM, Poveda G. 2014. Detection of long-term trends in monthly hydro-climatic series of Colombia through empirical mode decomposition. *Climatic Change* 123: 301-313. <https://doi.org/10.1007/s10584-013-1046-3>
- Chen D, Liu Z, Davis C, Gu Y. 2017. Dust radiative effects on atmospheric thermodynamics and tropical cyclogenesis over the Atlantic Ocean using WRF-Chem coupled with an AOD data assimilation system. *Atmospheric Chemistry and Physics* 17: 7917-7939. <https://doi.org/10.5194/acp-17-7917-2017>
- Connolly R, Soon W, Connolly M, Baliunas S, Berglund J, Butler CJ, Cionco RG, Elias AG, Fedorov VM, Harde H, Henry GW, Hoyt DV, Humlum O, Legates DR, Lüning S, Scafetta N, Solheim JE, Szarka L, Van-Loon H, Velasco-Herrera VM, Wilson RC, Yan H, Zhang W. 2021. How much has the Sun influenced Northern Hemisphere temperature trends? An ongoing debate. *Research in Astronomy and Astrophysics* 21: 131. <https://doi.org/10.1088/1674-4527/21/6/131>
- Dahmen ER, Hall MJ. 1990. Screening of hydrological data: Tests for stationarity and relative consistency. International Institute for Land Reclamation and Improvement, Wageningen.
- De A, Shreya S, Sarkar N, Maitra A. 2023. Time series trend analysis of rainfall and temperature over Kolkata and surrounding region. *Atmósfera* 37: 71-84. <https://doi.org/10.20937/ATM.53059>
- El-Geziry TM. 2022. Analysis of air temperature trends as a climate change indicator for Alexandria (Egypt). *Athens Journal of Sciences* 9: 239-256. <https://doi.org/10.30958/ajs.9-4-2>
- Eslava J. 1992. Perfil altitudinal de la temperatura media del aire en Colombia. *Earth Sciences Research Journal 1*: 37-52. Available at <https://revistas.unal.edu.co/index.php/esrj/article/view/31200> (accessed 2022 May 12).
- Friis-Christensen E, Lassen K. 1991. Length of the solar cycle: An indicator of solar activity closely associated with climate. *Science* 254: 698-700. <https://doi.org/10.1126/science.254.5032.698>
- Friis-Christensen E, Lassen K. 1994. Solar activity and global temperature. *International Astronomical Union Colloquium* 143: 339-347. <https://doi.org/10.1017/S0252921100024830>
- González-Rodríguez E, Villalobos H, Gómez-Muñoz VM, Ramos-Rodríguez A. 2015. Computational method for extracting and modeling periodicities in time series. *Open Journal of Statistics* 5: 604-617. <https://doi.org/10.4236/ojs.2015.56062>
- Hamed KH, Rao RA. 1998. A modified Mann-Kendall trend test for autocorrelated data. *Journal of Hydrology* 204: 182-196. [https://doi.org/10.1016/S0022-1694\(97\)00125-X](https://doi.org/10.1016/S0022-1694(97)00125-X)
- Hernández O. 2014. Intrusiones de polvo africano en la región Caribe de Colombia. *Gestión y Ambiente* 17: 11-29. Available at <https://revistas.unal.edu.co/index.php/gestion/article/view/43057> (accessed 2022 September 7)
- Hodson de Jaramillo E, Castaño J, Poveda G, Roldán G, Chavarriaga-Aguirre P. 2017. Seguridad alimentaria y nutricional en Colombia. In: Retos y oportunidades de la seguridad alimentaria y nutricional en las Américas: El punto de vista de las academias de ciencias. Inter-American Network of Academies of Sciences, Ciudad de México, 220-249.
- Hurtado-Montoya AF, Mesa-Sánchez ÓJ. 2015. Cambio climático y variabilidad espacio-temporal de la precipitación en Colombia. *Revista EIA* 12: 131-150. <https://doi.org/10.24050/reia.v12i24.879>
- IDEAM. 2011. Clasificación climática de Colombia. Grupo de Climatología y Agrometeorología Subdirección de Meteorología. II Congreso Nacional del Clima. Instituto de Hidrología, Meteorología y Estudios Ambientales. Available at <http://www.ideam.gov.co/documents/21021/21789/climas+%5BModo+de+compatibilidad%5D.pdf/d8c85704-a07a-4290-ba65-f2042ce99ff9> (accessed 2022 September 7).
- IDEAM. 2015. Atlas climatológico de Colombia. Instituto de Hidrología, Meteorología y Estudios Ambientales. Available at <http://www.ideam.gov.co/web/tiempo-y-clima/atlas> (accessed 2022 May 05).

- IDEAM. 2017. Tercera Comunicación Nacional de Colombia a la Convención Marco De Las Naciones Unidas Sobre Cambio Climático (CMNUCC). Instituto de Hidrología, Meteorología y Estudios Ambientales, Bogotá, Colombia. Available at <http://www.cambioclimatico.gov.co/resultados> (accessed 2022 December 11).
- Jones PD, Groisman PY, Coughlan M, Plummer N, Wang WC, Karl TR. 1990. Assessment of urbanization effects in time series of surface air temperature over land. *Nature* 347: 169-172. <https://doi.org/10.1038/347169a0>
- Künzel, H. 1962. M. Waldmeier: The sunspot-activity in the years 1610-1960. Zürich 1961: Verlag Schulthess u. Co. AG. Astronomische Nachrichten 286: 285-286. <https://doi.org/10.1002/asna.19622860613>
- Lamb WF, Wiedmann T, Pongratz J, Andrew R, Crippa M, Olivier JGJ, Wiedenhofer D, Mattioli G, Al-Khourdajie A, House J, Pachauri S, Figueroa M, Saheb Y, Slade R, Hubacek K, Sun L, Khan-Ribeiro S, Khennas S, De la Rue du Can S, Chapungu L, Davis SJ, Bashmakov I, Dai H, Dhakal S, Tan X, Geng Y, Gu B, Minx J. 2021. A review of trends and drivers of greenhouse gas emissions by sector from 1990 to 2018. *Environmental Research Letters* 16: 073005. <https://doi.org/10.1088/1748-9326/abee4e>
- León GE. 2000. Variabilidad y tendencia de la temperatura del aire en las cuatro principales ciudades de Colombia. *Meteorología Colombiana* 2: 81-86. Available at http://168.176.14.11/fileadmin/content/geociencias/revista_meteorologia_colombiana/numero02/02_11.pdf (accessed 2023 February 1).
- León GE, Zea-Mazo JA, Eslava-Ramírez JA. 2000. Circulación general del trópico y la Zona de Confluencia Intertropical en Colombia. *Meteorología Colombiana* 1: 31-38. Available at: http://168.176.14.11/fileadmin/content/geociencias/revista_meteorologia_colombiana/numero01/01_05.pdf (accessed 2023 January 22).
- Martín-Garzón A. 2021. Correlación entre la temperatura superficial del sensor Modis y la temperatura media del aire en el Departamento de la Guajira, Colombia. M.Sc. tesis. Universidad Antonio Nariño, Colombia.
- Mateus C, Potito A. 2022. Long-term trends in daily extreme air temperature indices in Ireland from 1885 to 2018. *Weather and Climate Extremes* 36: 100464. <https://doi.org/10.1016/j.wace.2022.100464>
- Meisel-Roca A, Pérez-Valbuena GJ. 2006. Documentos de trabajo sobre economía regional. Geografía física y poblamiento en la costa Caribe colombiana 73. Banco de la República, Cartagena de Indias, 79 pp. <https://doi.org/10.32468/dtsuru.73>
- Mohalfi S, Bedi HS, Krishnamurti TN, Cocke SD. 1998. Impact of shortwave radiative effects of dust aerosols on the summer season heat low over Saudi Arabia. *Monthly Weather Review* 126: 3153-3168. [https://doi.org/10.1175/1520-0493\(1998\)126<3153:IOS-REO>2.0.CO;2](https://doi.org/10.1175/1520-0493(1998)126<3153:IOS-REO>2.0.CO;2)
- Morales-Acuña E, Torres CR, Delgadillo-Hinojosa F, Linero-Cueto JR, Santamaría-del-Ángel E, Castro R. 2019. The Baja California Peninsula, a significant source of dust in northwest Mexico. *Atmosphere* 10: 582. <https://doi.org/10.3390/atmos10100582>
- Morales-Acuña E, Linero-Cueto JR, Canales FA. 2021. Assessment of Precipitation Variability and Trends Based on Satellite Estimations for a Heterogeneous Colombian Region. *Hydrology*. <https://doi.org/10.3390/hydrology8030128>
- NOAA. 2005a. The Southern Oscillation Index (SOI). National Weather Service/Climate Prediction Center, National Oceanic and Atmospheric Administration. Available at https://www.cpc.ncep.noaa.gov/products/analysis_monitoring/ensocycle/soi.shtml (accessed 2022 January 18).
- NOAA. 2005b North Atlantic Oscillation (NAO). National Weather Service/Climate Prediction Center, National Oceanic and Atmospheric Administration. Available at <https://www.cpc.ncep.noaa.gov/products/precip/CWlink/pna/nao.shtml> (accessed 2022 January 18).
- NOAA. 2018. Multivariate ENSO Index Version 2 MEI. v2. Physical Sciences Laboratory, National Oceanic and Atmospheric Administration. Available at <https://psl.noaa.gov/enso/mei/> (accessed 2022 January 18).
- Ochoa A, Poveda G. 2008. Distribución espacial de señales de cambio climático en Colombia. In: XXII Congreso Latinoamericano de Hidráulica. Cartagena de Indias. Available at <https://repositorio.unal.edu.co/handle/unal/7763> (accessed 2022 October 18).
- Orozco-Rodríguez WJ. 2021. Intrusiones de polvo desde la península de la Guajira y sus efectos en las concentraciones de clorofila del sistema de surgencia de la Guajira. B.Sc. tesis. Universidad de Bogotá Jorge Tadeo Lozano, Colombia.
- Ortiz-Tánchez E, Ebeling W, Lanius K. 2002. MEI, SOI and mid-range correlations in the onset of El Niño-Southern Oscillation. *Physica A: Statistical Mechanics and its Applications* 310: 509-520. [https://doi.org/10.1016/S0378-4371\(02\)00812-9](https://doi.org/10.1016/S0378-4371(02)00812-9)

- Pabón-Caicedo JD, Eslava-Ramírez JA, Gómez-Torres RE. 2001. Generalidades de la distribución espacial y temporal de la temperatura del aire y de la precipitación en Colombia. *Meteorología Colombiana* 4: 47-59. Available at http://168.176.14.11/fileadmin/content/geociencias/revista_meteorologia_colombiana/numero04/04_05.pdf (accessed 2022 January 18).
- Pabón-Caicedo JD. 2003. El cambio climático global y su manifestación en Colombia. *Cuadernos de Geografía: Revista Colombiana de Geografía* 12: 111-119. Available at <https://revistas.unal.edu.co/index.php/rcg/article/view/10277> (accessed 2022 January 18).
- Poleo D, Briceño CJ. 2014. La intrusión de polvo del Sahara y del Sahel en la capa límite atmosférica del Mar Caribe: episodio de agosto 2013. *Tópicos Meteorológicos y Oceanográficos* 13: 68-89. Available at <http://cglobal.imn.ac.cr/documentos/revista/topicosmet20142/index.html> (accessed 2022 January 18).
- Poveda G. 2004. La hidroclimatología de Colombia: una síntesis desde la escala interdecadal hasta la escala diurna. *Revista de la Academia Colombiana de Ciencias Exactas, Físicas Y Naturales* 28: 201-222. [https://doi.org/10.18257/raccefyn.28\(107\).2004.1991](https://doi.org/10.18257/raccefyn.28(107).2004.1991)
- Puertas-Orozco OL, Carvajal-Escobar Y. 2008. Incidence of El Niño-Southern Oscillation in the precipitation and the temperature of the air in Colombia, using Climate Explorer. *Ingeniería y Desarrollo* 23: 104-118. Available at <http://hdl.handle.net/10584/3941> (accessed 2022 March 8).
- Ramírez-Villegas J, Salazar M, Jarvis A, Navarro-Racines CE. 2012. A way forward on adaptation to climate change in Colombian agriculture: Perspectives towards 2050. *Climatic Change* 115: 611-628. <https://doi.org/10.1007/s10584-012-0500-y>
- Rangel-Buitrago N, Anfuso-Melfi G. 2013. Morfología, morfodinámica y evolución reciente en la Península de la Guajira, Caribe colombiano. *Revista de la Facultad de Ingeniería de la Universidad de Cartagena* 8: 7-24. Available at <https://hdl.handle.net/11227/5181> (accessed 2023 January 14).
- Rasmusson EM, Wang X, Ropelewski CF. 1990. The biennial component of ENSO variability. *Journal of Marine Systems* 1: 71-96. [https://doi.org/10.1016/0924-7963\(90\)90153-2](https://doi.org/10.1016/0924-7963(90)90153-2)
- Rodríguez-Rubio E. 2013. A multivariate climate index for the western coast of Colombia. *Advances in Geosciences* 33: 21-26. <https://doi.org/10.5194/adgeo-33-21-2013>
- Ruessink BG, van Enckevort IMJ, Kuriyama Y. 2004. Nonlinear principal component analysis of nearshore bathymetry. *Marine Geology* 203: 185-197. [https://doi.org/10.1016/S0025-3227\(03\)00334-7](https://doi.org/10.1016/S0025-3227(03)00334-7)
- Scholz M, Kaplan F, Guy CL, Kopka J, Selbig J. 2005. Nonlinear PCA: A missing data approach. *Bioinformatics* 21: 3887-3895. <https://doi.org/10.1093/bioinformatics/bti634>
- Scholz M. 2007. Analysing periodic phenomena by circular PCA. In: *Bioinformatics Research and Development, First International Conference (BIRD) 2007* (Hochreiter S, Wagner R, Eds.). Springer Berlin Heidelberg, Berlin, 38-47. https://doi.org/10.1007/978-3-540-71233-6_4
- Sen PK. 1968. Estimates of the regression coefficient based on Kendall's tau. *Journal of the American Statistical Association* 63: 1379-1389. <https://doi.org/10.1080/01621459.1968.10480934>
- Serna LM, Arias PA, Vieira SC. 2018. Las corrientes superficiales de chorro del Chocó y el Caribe durante los eventos de El Niño y El Niño Modoki. *Revista de la Academia Colombiana de Ciencias Exactas, Físicas y Naturales* 42: 410 - 421. <https://doi.org/10.18257/raccefyn.705>
- SILSO. 2015. Sunspot number graphics. Solar Influences Data Analysis Center, Sunspot Index and Long-term Solar Observations (SILSO). Available at <http://www.sidc.be/silso/ssngraphics> (accessed 2022 January 18).
- Slingo A, Ackerman TP, Allan RP, Kassianov EI, McFarlane SA, Robinson GJ, Barnard JC, Miller MA, Harries JE, Russell JE, Dewitte S. 2006. Observations of the impact of a major Saharan dust storm on the atmospheric radiation balance. *Geophysical Research Letters* 33: L24817. <https://doi.org/10.1029/2006GL027869>
- Spearman C. 1904. The proof and measurement of association between two things. *The American Journal of Psychology* 15: 72-101. <https://doi.org/10.2307/1412159>
- Theil H. 1950. A rank-invariant method of linear and polynomial regression analysis, 1-2; confidence regions for the parameters of linear regression equations in two, three and more variable. *Indagationes Mathematicae* 1: 385-392. Available at <https://ir.cwi.nl/pub/18446> (accessed 2022 September 8).
- Vanegas-Chamorro M, Villicaña-Ortíz E, Arrieta-Viana L. 2015. Cuantificación y caracterización de la radiación solar en el departamento de La Guajira-Colombia mediante el cálculo de transmisibilidad atmosférica. *Prospectiva* 13: 54-63. <https://doi.org/10.15665/rp.v13i2.487>

- Velasco-Herrera VM, Soon W, Legates DR. 2021. Does machine learning reconstruct missing sunspots and forecast a new solar minimum? *Advances in Space Research* 68: 1485-1501. <https://doi.org/10.1016/j.asr.2021.03.023>
- Vuille M, Bradley RS, Werner M, Keimig F. 2003. 20th century climate change in the tropical Andes: Observations and model results. *Climatic Change* 59: 75-99. <https://doi.org/10.1023/A:1024406427519>
- WMO. 2017. WMO Guidelines on the Calculation of Climate Normals (WMO-No.1203). World Meteorological Organization, Geneva.
- Wolter K, Timlin MS. 2011. El Niño/Southern Oscillation behaviour since 1871 as diagnosed in an extended multivariate ENSO index (MEI.ext). *International Journal of Climatology* 31: 1074-1087. <https://doi.org/10.1002/joc.2336>
- Yepes J, Poveda G, Mejía JF, Moreno L, Rueda C. 2019. CHOCO-JEX: A research experiment focused on the Chocó Low-Level Jet over the far eastern Pacific and western Colombia. *Bulletin of the American Meteorological Society* 100: 779-796. <https://doi.org/10.1175/BAMS-D-18-0045.1>
- Zar JH. 1972. Significance testing of the spearman rank correlation coefficient. *Journal of the American Statistical Association* 67: 578-580. <https://doi.org/10.1080/01621459.1972.10481251>

SUPPLEMENTARY MATERIAL

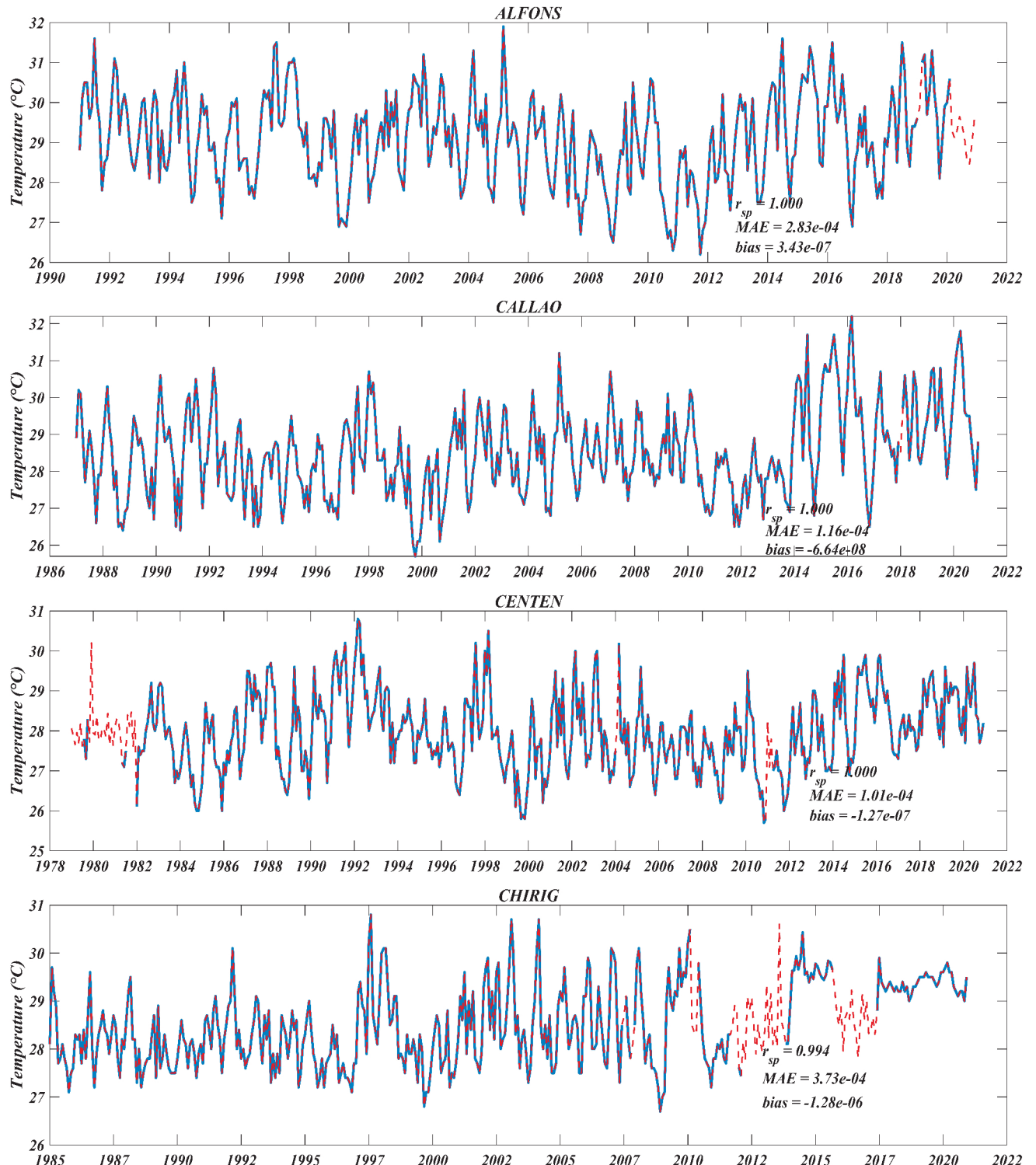


Fig. S1. Statistical metrics of Spearman correlation coefficient of reconstructed time series by nonlinear principal component analysis (NLPCA) and original time series in Cesar.

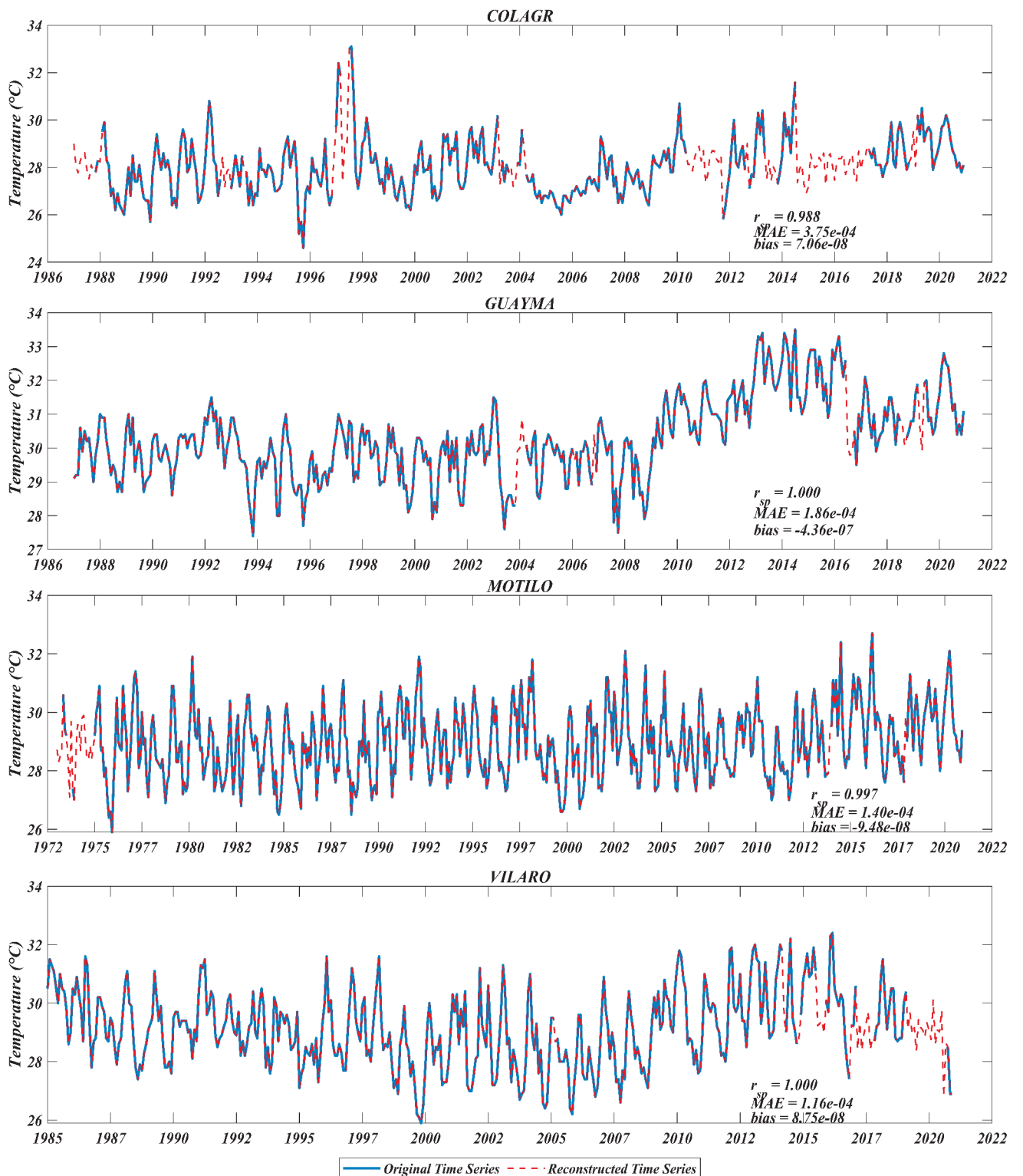


Fig. S1. Statistical metrics of Spearman correlation coefficient of reconstructed time series by nonlinear principal component analysis (NLPCA) and original time series in Cesar.

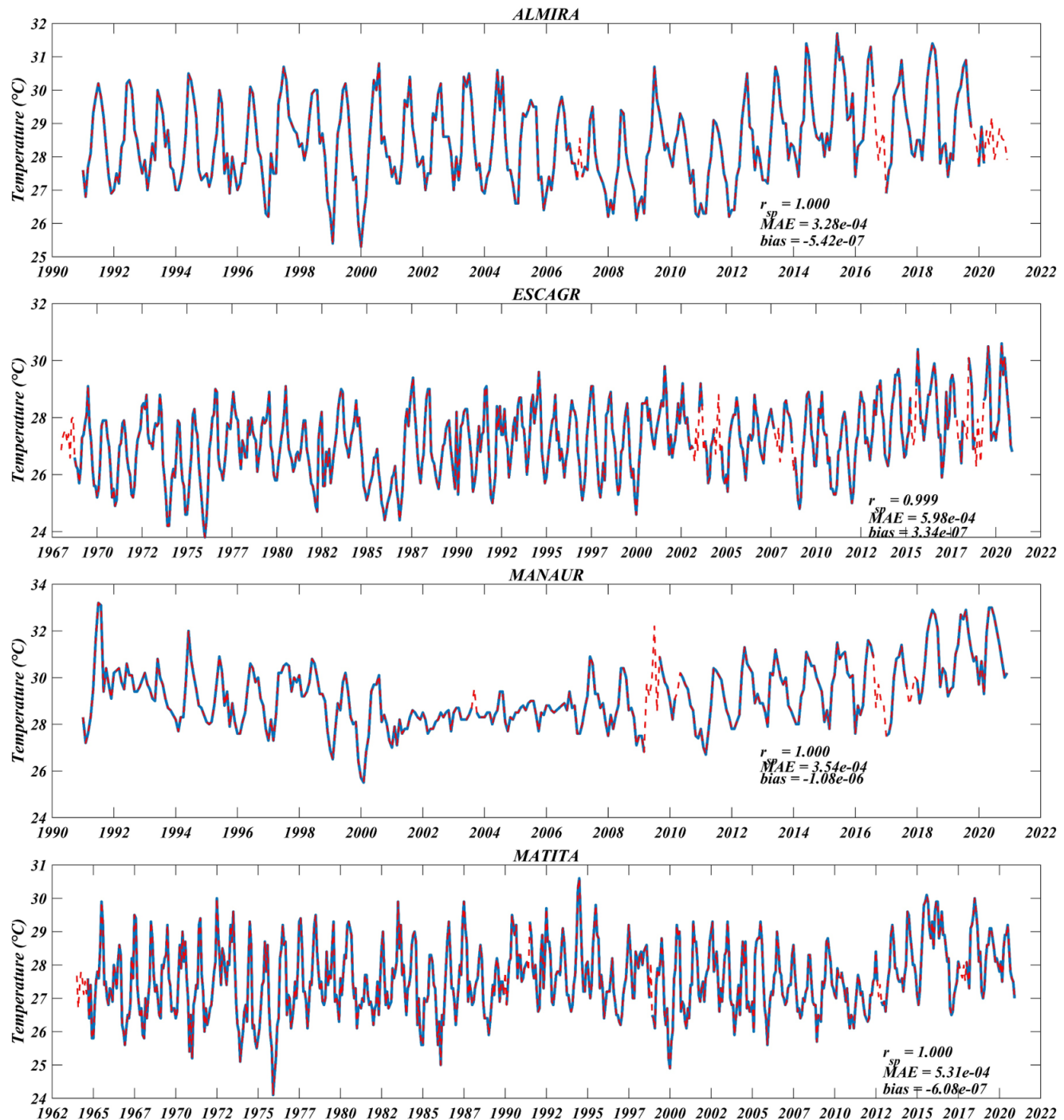


Fig. S2. Statistical metrics of Spearman correlation coefficient of reconstructed time series by nonlinear principal component analysis (NLPCA) and original time series in La Guajira.

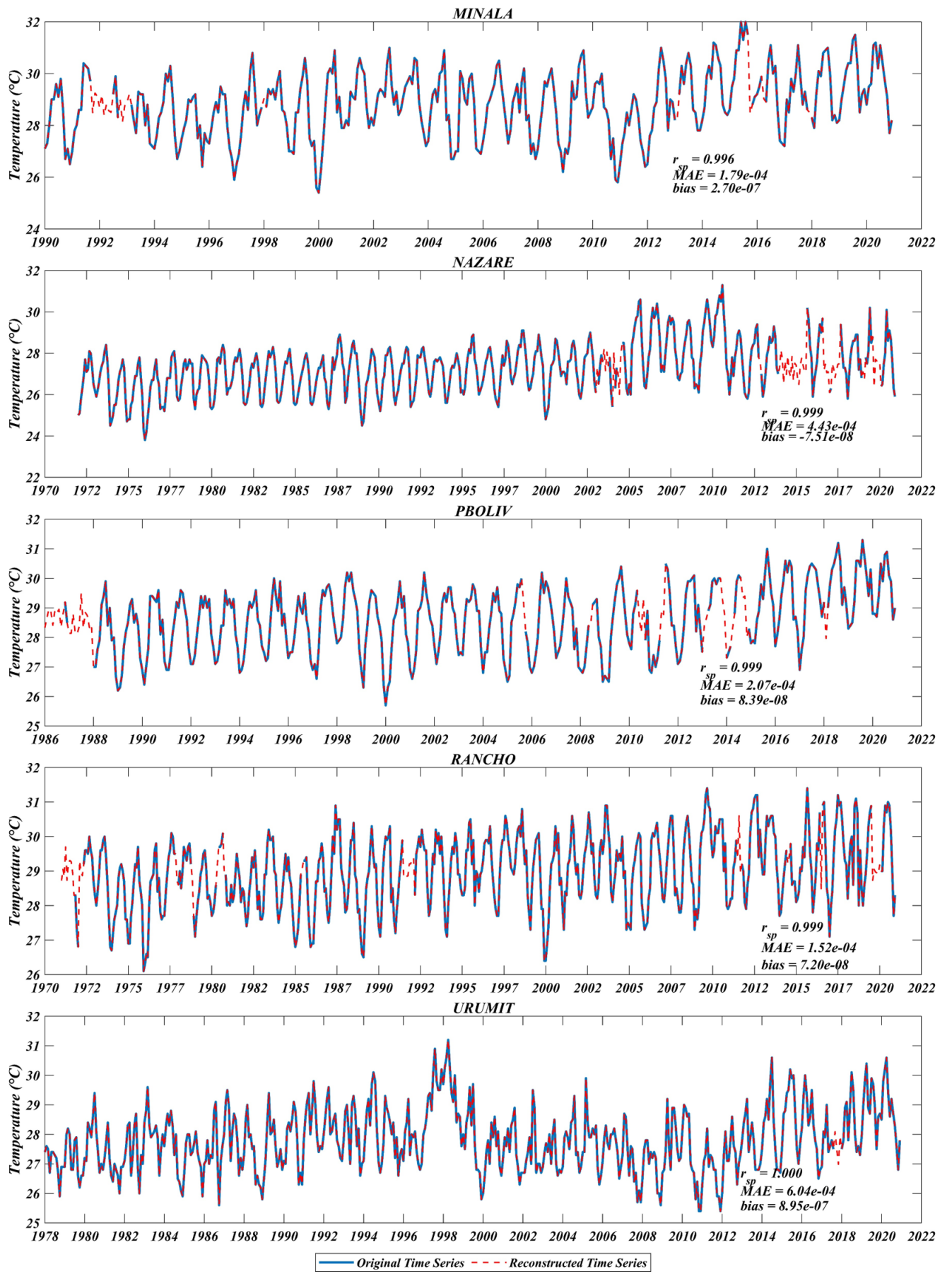


Fig. S2. Statistical metrics of Spearman correlation coefficient of reconstructed time series by nonlinear principal component analysis (NLPCA) and original time series in La Guajira.

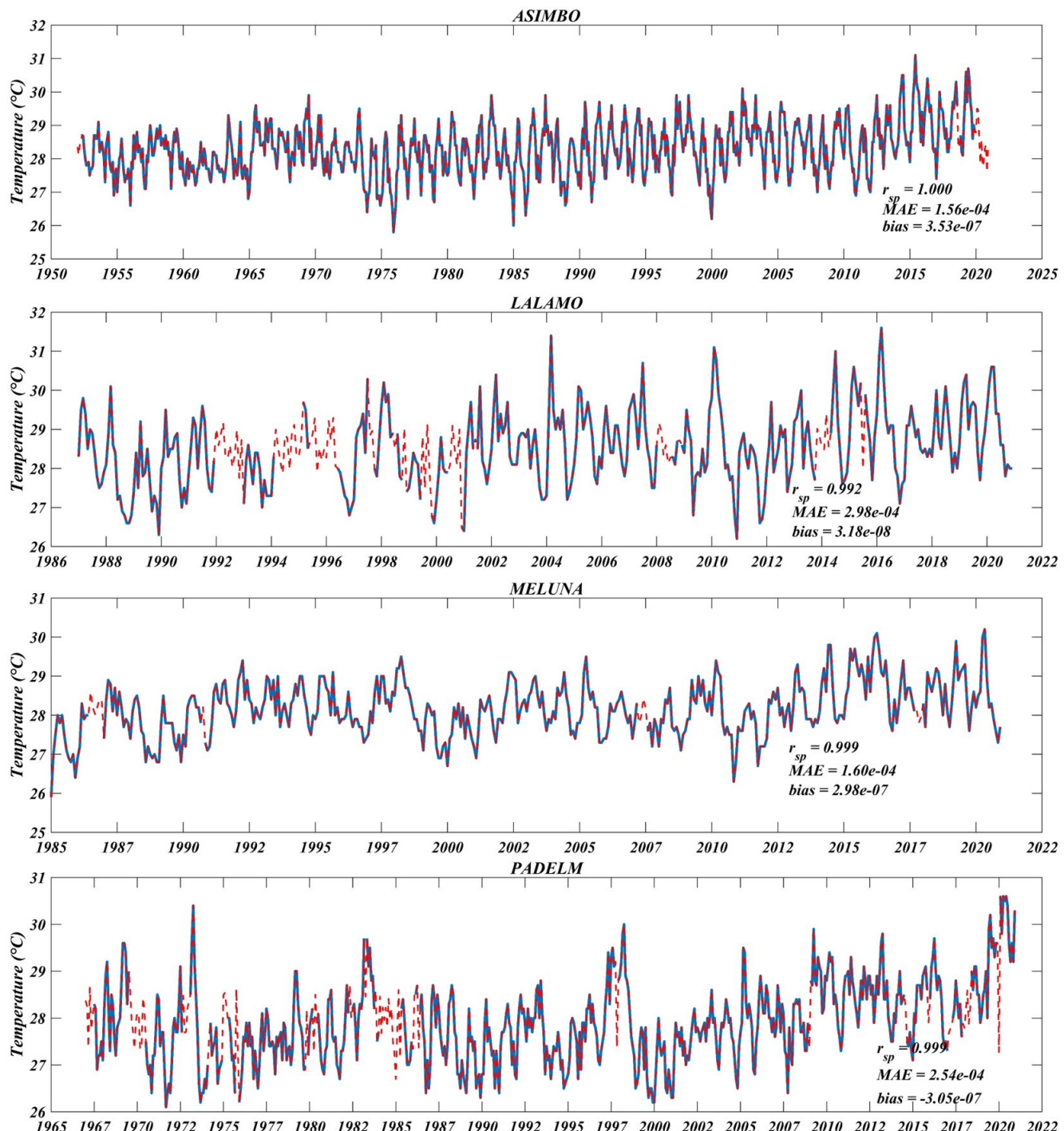


Fig. S3. Statistical metrics of Spearman correlation coefficient of reconstructed time series by nonlinear principal component analysis (NLPCA) and original time series in Magdalena.

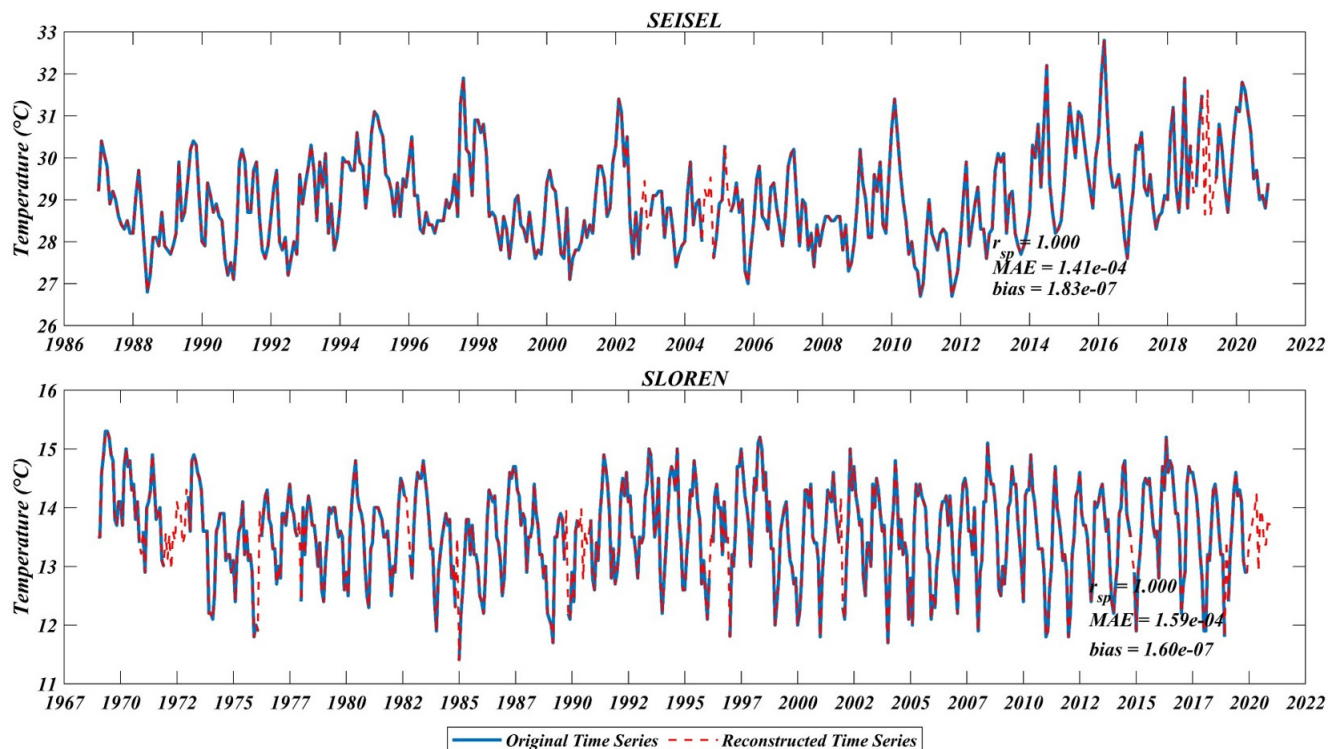


Fig. S3. Statistical metrics of Spearman correlation coefficient of reconstructed time series by nonlinear principal component analysis (NLPCA) and original time series in Magdalena.